AIP Applied Physics Letters

+Capacitance-voltage characteristics of Bi Fe O 3／Sr Ti O 3／Ga N heteroepitaxial structures

S. Y. Yang, Q. Zhan, P. L. Yang, M. P. Cruz, Y. H. Chu, R. Ramesh, Y. R. Wu, J. Singh, W. Tian, and D. G. Schlom

Citation: Applied Physics Letters **91**, 022909 (2007); doi: 10.1063/1.2757089
View online: http://dx.doi.org/10.1063/1.2757089
View Table of Contents: http://scitation.aip.org/content/aip/journal/apl/91/2?ver=pdfcov
Published by the AIP Publishing

Capacitance-voltage characteristics of $BiFeO_3/SrTiO_3/GaN$ heteroepitaxial structures

S. Y. Yang,[a] Q. Zhan, P. L. Yang, M. P. Cruz,[b] Y. H. Chu, and R. Ramesh
Department of Materials Science and Engineering & Department of Physics, University of California, Berkeley, California 94720

Y. R. Wu and J. Singh
Department of Electrical Engineering and Computer Science, University of Michigan, Ann Arbor, Michigan 48109

W. Tian and D. G. Schlom
Department of Materials Science and Engineering, Pennsylvania State University, University Park, Pennsylvania 16802

(Received 30 March 2007; accepted 19 June 2007; published online 11 July 2007)

The authors report the integration of multiferroic $BiFeO_3$ films with the semiconductor GaN using liquid-delivery metal-organic chemical-vapor deposition. Epitaxial $BiFeO_3$ films were deposited via interface control using $SrTiO_3$ buffer/template layers. The growth orientation relationship was found to be $(111)[1\bar{1}0]BiFeO_3 \| (111)[1\bar{1}0]SrTiO_3 \| (0001)[11\bar{2}0]GaN$, with in-plane 180° rotational twins. The *C-V* characteristics of a $Pt/BiFeO_3/SrTiO_3/GaN$ capacitor exhibited hysteresis with a memory window of ~3 V at a sweeping voltage of ±30 V. © *2007 American Institute of Physics*. [DOI: 10.1063/1.2757089]

Considerable research on the integration of ferroelectric thin films with semiconductors has been performed,[1–6] leading to various device applications including memory storage devices, i.e., ferroelectric field-effect transistors and optoelectronic devices. This integration enables the performance of currently existing devices to be tailored, and moreover, is the driving force for future multifunctional semiconductor devices. In this respect, it has been demonstrated that the integration of epitaxial ferroelectric/piezoelectric films with Si can be achieved using a perovskite $SrTiO_3$ template/buffer layer grown by molecular-beam epitaxy.[7–9]

Recently, ferroelectric heterostructures on GaN have been investigated due to the distinct advantages of GaN: high electron mobility, high breakdown voltage, and chemical and thermal stability. For the development of high-temperature device applications on GaN, the availability of a stable ferroelectric layer at high temperature is an essential requirement. Perovskite $BiFeO_3$ has been intensively studied because of its large ferroelectric polarization and high ordering temperature (ferroelectric Curie temperature $T_C \sim 1100$ K), which enables $BiFeO_3$ to be the most promising candidate as a ferroelectric layer for high temperature device applications.

GaN has a wurtzite structure with lattice constants of $a=3.186$ Å and $c=5.178$ Å, whereas $BiFeO_3$ has a rhombohedrally distorted perovskite structure with a pseudocubic lattice constant of 3.96 Å. Pseudocubic indices are used for $BiFeO_3$ throughout this letter. Considering the design of metal-ferroelectrics-insulator-semiconductor (MFIS) structures, it is important to employ a buffer layer with a high dielectric constant to minimize the drop in external field across this layer. The high dielectric constant (~300) of $SrTiO_3$ compared with that of $BiFeO_3$ (~100) allows the external field to be applied to the ferroelectric $BiFeO_3$ layer.

$BiFeO_3$ was epitaxially grown on (0001) GaN with the Ga terminated face using a thin intermediate (111) $SrTiO_3$ buffer layer about 2 nm thick. Following prior work in which such epitaxy was achieved using thick $SrTiO_3$ and TiO_2 intermediate layers,[10] we minimized the thickness of these intermediate buffer layers and attempted, via a topotactic reaction, to completely eliminate the TiO_2 layer. Details of the *in situ* and *ex situ* structural characterizations of this epitaxial buffer layer are shown in Fig. 1. The (111) $SrTiO_3$ buffer layer in the present work was achieved by scaling the (100) TiO_2 buffer layer down to a thickness of 6 Å [Fig. 1(b)]. The total dose of Ti in a 0.6 nm thick TiO_2 layer corresponds to five Ti monolayers in the $Ti–SrO_3–Ti–SrO_3–\cdots$ layering sequence of a (111)-oriented $SrTO_3$ film. On top of this TiO_2 layer a dose of Sr corresponding to four SrO_3 monolayers in (111)-oriented $SrTiO_3$ was deposited to start the reaction with the underlying TiO_2 to form (111) $SrTiO_3$. The substrate temperature was held at ~630 °C to promote the reaction between the TiO_2 and SrO layers [Fig. 1(c)]. The result was an epitaxially (111) oriented $SrTiO_3$ thin layer on the (0001) surface of GaN. Although rough at the surface, such a thin (~2 nm) (111) $SrTiO_3$ layer provides a viable template for the overlaying growth of (111) oriented $BiFeO_3$. X-ray characterization [Figs. 1(d) and 1(e)] indicates that the epitaxial orientation relationship is $(111)[1\bar{1}0]SrTiO_3 \| (0001)[11\bar{2}0]GaN$, identical to that found for thicker $SrTiO_3/TiO_2$ buffer layers. The $SrTiO_3$ film possesses a high degree of structural quality indicated by a 0.13° full width at half maximum of the rocking curve of the 111 $SrTiO_3$ reflection. A high-resolution transmission electron microscopy (HRTEM) image [Fig. 1(f)], however, reveals that approximately 2 ML of TiO_2 at the interface (between the two dashed lines in the image) were not completely converted to $SrTiO_3$.

The growth of $BiFeO_3$ films by metal-organic chemical-vapor deposition is described in detail elsewhere.[11] In this study, triphenylbismuth $[Bi(Ph)_3]$ and tris(2,2,6,6-

[a]Electronic mail: syyang@berkeley.edu
[b]Also at Centro de Ciencias de la Materia Condensada, Universidad Nacional Autónoma de México, Km 107 Caretera Tijuana-Ensenada, Ensenada, B.C., C.P. 22800, Mexico.

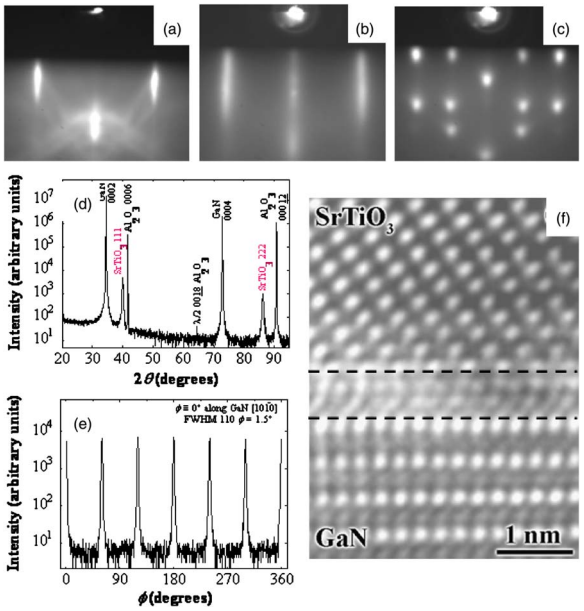

FIG. 1. (Color online) (a) Reflection high-energy electron diffraction (RHEED) image of bare (0001) GaN along the $[11\bar{2}0]$ azimuth. (b) RHEED image along the same azimuth after the growth of 0.6 nm of TiO_2 at T_{sub} =590 °C, which is identified to be along the [001] azimuth of the rutile polymorph of TiO_2 (Ref. 11). (c) RHEED image following the deposition of SrO at T_{sub}=630 °C. This pattern is identified to be along the [110] azimuth of (111) oriented.

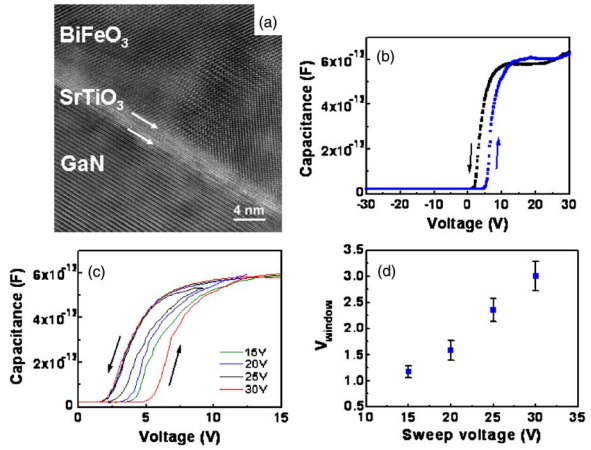

FIG. 2. (Color online) (a) Cross-sectional high-resolution transmission electron microscopy image of $BiFeO_3/SrTiO_3/GaN$ interfaces. (b) *C-V* characteristics of $BiFeO_3/SrTiO_3/GaN$ structures over a sweep range of ±30 V. (c) *C-V* curves measured at different sweep voltages (±15, ±20, ±25, and ±30 V). (d) The dependence of the memory window on sweep voltage.

tetramethyl-3,5-heptanedionate)iron $[Fe(thd)_3]$, dissolved in tetrahydrofuran, were selected as metal-organic precursors for $BiFeO_3$ film growth due to their clean thermal decomposition behavior. The thickness of the $BiFeO_3$ films used was 300 nm.

In order to make Ohmic contacts to *n*-GaN, the $BiFeO_3/SrTiO_3$ layers were partially etched with 50:1 buffered oxide etch (BOE) solution. Ti (15 nm)/Al (200 nm)/Ni (150 nm)/Au (150 nm) layers were successively deposited on the GaN surface in an electron-beam evaporator without breaking vacuum, followed by rapid thermal annealing at 600 °C for 35 s in 1 atm of N_2. Standard photolithography and lift-off processes were used to define 32 μm diameter Pt top electrodes on the $BiFeO_3$ film. Capacitance-voltage (*C-V*) characteristics were measured over a frequency range of 1 kHz–1 MHz using an HP 4194A impedance/gain-phase analyzer.

In the case of epitaxial (111) $BiFeO_3/(111)$ $SrTiO_3/n$-(0001) GaN/sapphire the polarization direction of $BiFeO_3$ lies along the ⟨111⟩ pseudocubic direction of the rhombohedral structure, leading to the most efficient carrier modulation of the underlying GaN surface. Moreover, the single ferroelectric domain in the (111)$BiFeO_3$ film allows for the possibility of controlling the device by excluding the intricate domain configuration in epitaxial $BiFeO_3$ films.[12] *P-E* hysteresis loops (not shown here for brevity) from a 300 nm thick $BiFeO_3$ film on $SrRuO_3$/2 nm $SrTiO_3$/GaN yield a $2P_r$ value of ~190 $\mu C/cm^2$. We note that this polarization value is consistent with theoretically calculated and experimentally observed values for (111) $BiFeO_3$ films on $SrTiO_3$ substrates.[13,14]

The field effect in a MFIS heterostructure is sensitive to interfacial states, which can be obscured by charge injection from the semiconductor into the ferroelectric layer. Therefore, in order to conclusively identify the exact mechanism of ferroelectric switching, it is important to evaluate the structural and chemical properties at the interfaces to rule out the possibility of charge injection. A HRTEM image showing the $BiFeO_3/SrTiO_3/GaN$ interfaces [Fig. 2(a)] was found to be clean and well defined, without any evidence of transition layers.

The *C-V* curves were measured by a voltage sweep from a positive bias to a negative bias (down sweep) followed by an opposite voltage sweeping direction (up sweep). In such a measurement, hysteresis between up- and down-sweep directions was observed, as shown in Fig. 2(b). In contrast to clockwise hysteresis direction caused by charge injection with the *n*-type semiconductor, counterclockwise hysteresis, as indicated by arrows in Fig. 2(b), demonstrates that the memory window is induced by the ferroelectric nature of the $BiFeO_3$ film.[15] The memory window measured at different applied sweep voltages showed the flatband voltage shifts with the magnitude of the sweep bias. The memory window increases linearly with applied voltage, reaching 3 V at ±30 V, as shown in Figs. 2(c) and 2(d). The time dependence of capacitance showed negligible retention loss up to 12 h with the write voltage of ±30 V.

To model the counterclockwise hysteresis loops, the charge control model was applied by solving the Poisson and drift-diffusion equations self-consistently.[16,17] The ferroelectric effect is taken into account by applying the boundary condition at the material interface as

$$\varepsilon_1 \mathbf{E} + \mathbf{P}_{\text{ferro}} = (1+\chi)\varepsilon_0 \mathbf{E} + \mathbf{P}_{\text{ferro}} = \varepsilon_2 \mathbf{E}_2, \tag{3}$$

where ε_1 and ε_2 are the linear dielectric constants of $BiFeO_3/SrTiO_3$ and $SrTiO_3/GaN$, respectively, and $\mathbf{P}_{\text{ferro}}$ is the polarization of the ferroelectric layer. The ferroelectric effects of $BiFeO_3$ and the negative polarization charge from GaN are taken into account by the above equation.

Considering the thickness (~2 nm) and high dielectric constant of $SrTiO_3$ compared with $BiFeO_3$, the total capacitance can be approximated to be that of $BiFeO_3$ (C_{BFO}). The effective dielectric constant extracted is approximately $90-95\varepsilon_0$ in the accumulation region for different voltage ranges. From the measured *C-V* curves, we have observed a shift of the threshold voltage towards positive values . Figure 3(a) shows the measured and simulated *C-V* curves

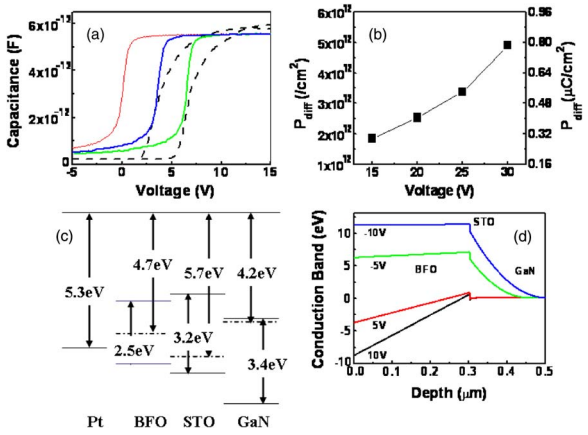

FIG. 3. (Color online) (a) Simulated *C-V* curves of $BiFeO_3/SrTiO_3/GaN$. The red solid line is the ideal *C-V* curve without any interface charge. The blue and green solid lines are calculated *C-V* curves containing different values of interface charge, -5.7×10^{12} and -1.06×10^{13} cm^{-2}, respectively. The dashed line is the measured *C-V* curve from experiment. (b) The simulated switched polarization charge vs sweep voltage. (c) Schematic of the idealized band diagram for Pt, $BiFeO_3$, $SrTiO_3$, and GaN before contact, where the Fermi energy of $BiFeO_3$ was assumed to lie in the middle of the band gap because of the lack of any published data. (d) The conduction band profile for different applied voltages.

in which the expected *C-V* curves are plotted by the solid lines for no interface charge or polarization charge. As shown in Fig. 3(a), however, the measured threshold voltages for the down and up loops are shifted by approximately 3–6 V. From fitting the experimental results, this corresponds to approximately 5.7×10^{12}–1.06×10^{13} cm^{-2} negative interface charges at either the $BiFeO_3/SrTiO_3$ or $SrTiO_3/GaN$ interface. The source of negative charges may come from a combination of ferroelectric polarization charge and negative GaN polar charges of the Ga terminated face. Ideally, GaN has a net negative surface polarization charge of 3.4 μC/cm^2 ($\sim2.0\times10^{13}$ cm^{-2}) for the Ga-faced buffer layer.[18] For a positive applied voltage in the accumulation region, it is reasonable to assume that the ferroelectric is switched to positive polarization at the $BiFeO_3/SrTiO_3$ interface to compensate the positive electric field. Therefore, the combination of these polar charges shows a 3–6 V threshold voltage shift for the up and down sweeps.

Figure 3(b) shows the fitted values of switched polarization versus different sweep voltage values. The results show a maximum of 0.76 μC/cm^2 ferroelectric polarization switched for the 30 V voltage sweep, which is only 1% of the maximum saturated polarization charge. Nonetheless, the operating window is 3 V, which is comparable to other work[19] and has promise for nonvolatile field effect devices.

Our simulations show that the channel charges are depleted in the negative bias region, as shown in Fig. 3(d). Because of the larger dielectric constant of $BiFeO_3$ compared to GaN and the ferroelectric effect which tends to reduce the band bending of the $BiFeO_3$ layer, the applied voltage is mainly dropped across the GaN layer so that the polarization of the $BiFeO_3$ is hardly switched due to the small external electric field. The fixed negative interface charge also provides a positive electric field in the $BiFeO_3$ layer so that in spite of the large applied bias it is hard to reach its negative coercive field.

For positive bias conditions, although the external electric field must be large to cause switching of the ferroelectric domain, the internal electric field needs to be large enough to cause switching of both the linear and ferroelectric polarizations. The internal electric field can be simply expressed as

$$E_{\text{int}} = \chi E + \frac{P_{\text{ferro}}}{\varepsilon_0}.$$

Due to the large band gap of GaN, for MFIS structures involving GaN, the insulator barrier of the ferroelectric might not be large enough to prevent leakage. Should the quasi-Fermi level be placed over the barrier, leakage will result. This would make it hard to build up enough internal fields for domain switching.

This research poses several immediate questions to improve the device performance. The writing voltage of the device is still too high. Therefore, optimizing the $BiFeO_3$ layer thickness and increasing the doping concentration in the *n*-GaN layer could significantly improve the device performance. The writing speed of the device is also an important factor to investigate in the future.

In conclusion, we have demonstrated the integration of epitaxial $BiFeO_3$ films on the semiconductor GaN using 2 nm thick $SrTiO_3$ buffer layers. By performing careful *C-V* measurements and comparing them to simulated results, it was observed that the surface charge of the underlying GaN is modulated by polarization switching of the ferroelectric $BiFeO_3$ film.

This work is supported by the U.S. Department of Energy under Contract No. DE-AC02-05CH11231 and by ONR Grant Nos. N00014-04-1-0426 and N00014-06-1-0008 monitored by Colin Wood.

[1]S. Mathews, R. Ramesh, T. Venkatesan, and J. Benedetto, Science **276**, 238 (1997).
[2]W. P. Li, R. Zhang, Y. G. Zhou, J. Yin, H. M. Bu, Z. Y. Luo, B. Shen, Y. Shi, R. L. Jiang, S. L. Gu, Z. G. Liu, Y. D. Zheng, and Z. C. Huang, Appl. Phys. Lett. **75**, 2416 (1999).
[3]V. Fuflyigin, A. Osinsky, F. Wang, P. Vakhutinsky, and P. Norris, Appl. Phys. Lett. **76**, 1612 (2000).
[4]A. Posadas, J.-B. Yau, C. H. Ahn, J. Han, S. Gariglio, K. Johnston, K. M. Rabe, and J. B. Neaton, Appl. Phys. Lett. **87**, 171915 (2005).
[5]A. Masuda, S. Morita, H. Shigeno, A. Morimoto, T. Shimizu, J. Wu, H. Yaguchi, and K. Onabe, J. Cryst. Growth **189/190**, 227 (1998).
[6]F. Wang, V. Fuflyigin, and A. Osinsky, J. Appl. Phys. **88**, 1701 (2000).
[7]Y. Wang, C. Ganpule, B. T. Liu, H. Li, K. Mori, B. Hill, M. Wuttig, R. Ramesh, J. Finder, Z. Yu, R. Droopad, and K. Eisenbeiser, Appl. Phys. Lett. **80**, 97 (2005).
[8]J. Wang, H. Zheng, Z. Ma, S. Prasertchoung, M. Wuttig, R. Droopad, J. Yu, K. Eisenbeiser, and R. Ramesh, Appl. Phys. Lett. **85**, 2574 (2005).
[9]A. Lin, X. Hong, V. Wood, A. A. Verevkin, C. H. Ahn, R. A. McKee, F. J. Walker, and E. D. Specht, Appl. Phys. Lett. **78**, 2034 (2001).
[10]W. Tian, V. Vaithyanathan, D. G. Schlom, Q. Zhan, S. Y. Yang, Y. H. Chu, and R. Ramesh, Appl. Phys. Lett. **90**, 172908 (2007).
[11]S. Y. Yang, F. Zavaliche, L. Mohaddes-Ardabili, V. Vaithyanathan, D. G. Schlom, Y. J. Lee, Y. H. Chu, M. P. Cruz, Q. Zhan, T. Zhao, and R. Ramesh, Appl. Phys. Lett. **87**, 102903 (2005).
[12]F. Zavaliche, R. R. Das, D. M. Kim, C. B. Eom, S. Y. Yang, P. Shafer, and R. Ramesh, Appl. Phys. Lett. **87**, 182912 (2005).
[13]J. B. Neaton, C. Ederer, U. V. Waghmare, N. A. Spaldin, and K. M. Rabe, Phys. Rev. B **71**, 014113 (2005).
[14]J. F. Li, J. Wang, N. Wang, F. Bai, B. Ruette, A. P. Pyatakov, M. Wuttig, R. Ramesh, A. K. Zvezdin, and D. Viehland, Appl. Phys. Lett. **84**, 5261 (2004).
[15]Y. Fujisaki, T. Kijima, and H. Ishiwara, Appl. Phys. Lett. **78**, 1285 (2001).
[16]Y. Wu and J. Singh, Appl. Phys. Lett. **85**, 1223 (2004).
[17]Y. Wu, M. Singh, and J. Singh, J. Appl. Phys. **94**, 5826 (2003).
[18]O. Ambacher, J. Majewski, C. Miskys, A. Link, M. Hermann, M. Eickhoff, M. Stutzmann, F. Bernardini, V. Fiorentini, V. Tilak, B. Schaff, and L. F. Eastman, J. Phys.: Condens. Matter **14**, 3399 (2002).
[19]M. Liu, H. K. Kim, and J. Blachere, J. Appl. Phys. **91**, 5985 (2002).